AMERICAN JOURNAL OF PHYSIOLOGY
LUNG CELLULAR AND MOLECULAR PHYSIOLOGY

*Am J Physiol Lung Cell Mol Physiol* 327: L535–L546, 2024.
*First published August 19, 2024; doi:10.1152/ajplung.00058.2024*

RESEARCH ARTICLE

*Alveolar Biology, Pulmonary Surfactant, and Beyond*

# Comparative biophysical study of clinical surfactants using constrained drop surfactometry

**Yi Y. Zuo**[1,2]

[1]*Department of Mechanical Engineering, University of Hawaii at Manoa, Honolulu, Hawaii, United States and* [2]*Department of Pediatrics, John A. Burns School of Medicine, University of Hawaii, Honolulu, Hawaii, United States*

## Abstract

Surfactant replacement therapy is crucial in managing neonatal respiratory distress syndrome (RDS). Currently licensed clinical surfactants in the United States and Europe, including Survanta, Infasurf, Curosurf, and Alveofact, are all derived from bovine or porcine sources. We conducted a comprehensive examination of the biophysical properties of these four clinical surfactant preparations under physiologically relevant conditions, using constrained drop surfactometry (CDS). The assessed biophysical properties included the adsorption rate, quasi-static and dynamic surface activity, resistance to surfactant inhibition by meconium, and the morphology of the adsorbed surfactant films. This comparative study unveiled distinct in vitro biophysical properties of these clinical surfactants and revealed correlations between their chemical composition, lateral film structure, and biophysical functionality. Notably, at 1 mg/mL, Survanta exhibited a significantly lower adsorption rate compared with the other preparations at the same surfactant concentration. At 10 mg/mL, Infasurf, Curosurf, and Survanta all demonstrated excellent dynamic surface activity, whereas Alveofact exhibited the poorest quasi-static and dynamic surface activity. The suboptimal surface activity of Alveofact is found to be correlated with its unique monolayer-predominant morphology, in contrast to other surfactants forming multilayers. Curosurf, in particular, showcased superior resistance to biophysical inhibition by meconium compared with other preparations. Understanding the diverse biophysical behaviors of clinical surfactants provides crucial insights for precision and personalized design in treating RDS and other respiratory conditions. The findings from this study contribute valuable perspectives for the development of more efficacious and fully synthetic surfactant preparations.

**NEW & NOTEWORTHY** A thorough investigation into the biophysical properties of four animal-derived clinical surfactant preparations was conducted through constrained drop surfactometry under physiologically relevant conditions. This comparative study unveiled unique in vitro biophysical characteristics among these clinical surfactants, establishing correlations between their chemical composition, lateral film structure, and biophysical functionality. The acquired knowledge offers essential insights for the precise and personalized design of clinical surfactant for the treatment of respiratory distress syndrome and other respiratory conditions.

*constrained drop surfactometry; pulmonary surfactant; respiratory distress syndrome; surface tension; surfactant replacement therapy*

## INTRODUCTION

Surfactant replacement therapy plays a pivotal role in managing neonatal respiratory distress syndrome (RDS) (1, 2). Despite the increasing utilization of noninvasive respiratory support, such as continuous positive airway pressure (CPAP), during the delivery of preterm infants, which gradually reduces the necessity for prophylactic surfactant, rescue surfactant remains the primary intervention for infants exhibiting clinical signs of RDS (3, 4). Currently, all surfactant preparations clinically used to treat infants with RDS are derived from animals, either bovine or porcine sources (5). Understanding the correlation between phospholipid/protein composition and the biophysical function of these clinical surfactants contributes to the development of more efficacious and fully synthetic surfactant preparations (6).

The most important biophysical properties of pulmonary surfactant include rapid phospholipid adsorption onto the air-water surface to reach an equilibrium surface tension of 22–25 mN/m, and the ability to decrease surface tension to low values upon compression of the adsorbed surfactant film (7, 8). The first direct quantitative surface tension measurement of compressed pulmonary surfactant film was performed by Clements in 1957 using a modified Langmuir film

Correspondence: Y. Y. Zuo (yzuo@hawaii.edu).
Submitted 16 February 2024 / Revised 16 June 2024 / Accepted 12 August 2024

balance (9). He demonstrated that saline extracts from rat, cat, and dog lungs decreased the surface tension from 46 to 10 mN/m when the surfactant film was compressed in a Langmuir film balance. Avery and Mead later applied Clements' method to measure the surface tension of postmortem airway lavage fluids from infants who succumbed to premature birth and other causes (10). Notably, premature infants' airway lavage exhibited a minimum surface tension ranging from 20 to 40 mN/m, considerably higher than infants who died from other causes. This revelation unveiled the true pathophysiology of what was then termed hyaline membrane disease, now recognized as RDS. Building upon Clements' pioneering work, subsequent research revealed surface tensions lower than 5 mN/m for rat and human surfactants using the same in vitro technique (11). In 1976, Schürch, Goerke, and Clements confirmed the relevance of these in vitro surface tension measurements to lung physiology (12). Using a microdroplet technique, they conducted the first in situ alveolar surface tension measurements in excised rat lungs. Their findings indicated a decrease in alveolar surface tension from 20 to 9 mN/m when the excised lung was deflated by 25% of the total lung capacity to its functional residual capacity at 37°C (12).

Although the Langmuir film balance serves as a straightforward interfacial model and an easily applicable technique for in vitro biophysical assays, it does have limitations in comprehensively assessing the biophysical properties of pulmonary surfactant (7). Its relatively large size hinders the thorough study of adsorbed surfactant films and poses challenges in maintaining precise environmental conditions, such as controlling the core body temperature at 37°C and sustaining 100% relative humidity. Consequently, it falls short in simulating the intra-alveolar environment. The Langmuir film balance is best suited for determining quasi-static surface properties, as rapid barrier oscillations induce waves that disrupt surface tension measurements with a Wilhelmy plate. A critical drawback is the susceptibility to film leakage, leading to the premature collapse of the surfactant film. To overcome these technical limitations, newer in vitro biophysical techniques have been developed for assessing pulmonary surfactant, including pulsating bubble surfactometry (PBS) (13), captive bubble surfactometry (CBS) (14), and constrained drop surfactometry (CDS) (15, 16). A comprehensive discussion of the advantages and disadvantages of these in vitro methods can be found in a recent review (17).

Here, we present a comparative study of the biophysical properties of four clinical surfactant preparations using a novel droplet-based surface tensiometry technique known as CDS (15, 16). Developed within our laboratory, CDS combines the strengths of the Langmuir film balance, PBS, and CBS, while mitigating the drawbacks associated with these methods in the study of pulmonary surfactants (17). Serving as an ideal in vitro model for investigating adsorbed surfactant films, CDS minimizes sample consumption (<10 μL per measurement) and, through system miniaturization, faithfully replicates the intra-alveolar microenvironment of pulmonary surfactants under physiologically relevant conditions (17). CDS overcomes the concentration limitations of CBS in studying adsorbed surfactant films (18) and provides a leakage-proof environment, similar to CBS, conducive to the examination of low surface tensions. In addition, we have pioneered innovative subphase replacement and in situ Langmuir–Blodgett (LB) transfer techniques, enabling direct atomic force microscopy (AFM) imaging of the ultrastructure and topography of adsorbed pulmonary surfactant films with submicron resolutions (16, 19). Using CDS, we conducted a comprehensive examination of the biophysical properties of four clinical surfactants under physiologically relevant conditions. These properties encompassed the adsorption rate, quasi-static and dynamic surface activity, resistance to surfactant inhibition by meconium, and the morphology of the adsorbed surfactant films. This comparative study unveiled correlations between the composition of a clinical surfactant and its biophysical functionality, providing valuable insights for the development of more efficacious and fully synthetic surfactant preparations.

## MATERIALS AND METHODS

### Materials

All four clinical surfactant preparations examined in this study were animal-derived natural surfactants. Despite variations in their manufacturing processes, all of them involved organic extraction, which eliminates the hydrophilic protein [surfactant protein A (SP-A)] and reduces the content of the hydrophobic proteins [surfactant protein B (SP-B) and surfactant protein C (SP-C)] (20, 21). The detailed chemical compositions of these clinical surfactants have been thoroughly documented (20–24). In particular, Calfactant (Infasurf, ONY Biotech, Amherst, NY) was extracted from the bronchoalveolar lavage of newborn calves. It contained most of the hydrophobic components of natural pulmonary surfactant, including cholesterol. Poractant alfa (Curosurf, Chiesi Farmaceutici, Parma, Italy) was prepared from minced porcine lung tissue. In addition to organic extraction and centrifugation, the manufacturing process of Curosurf involves an additional step of removing all neutral lipids through gel chromatography. Beractant (Survanta, Abbott Laboratories, North Chicago, IL) was extracted from minced bovine lung tissues, with additional procedures to remove neutral lipids (mainly cholesterol) and to supplement with synthetic dipalmitoyl phosphatidylcholine (DPPC), palmitic acid, and tripalmitin. Bovactant (Alveofact, Lyomark Pharma, Oberhaching, Germany) was extracted from bovine lung lavage but underwent an additional lyophilizing step, necessitating resuspension before administration. Figure 1 depicts the major lipid and protein compositions of these clinical surfactants (20–24). All four clinical surfactants were stored frozen at −20°C in sterilized vials at their original phospholipid concentrations. On the day of the experiment, each surfactant was allowed to gradually thaw to room temperature and then diluted to 1, 5, and 10 mg phospholipids/mL, respectively, using a saline buffer of 0.9% NaCl, 1.5 mM $CaCl_2$, and 2.5 mM HEPES, adjusted to pH 7.0 with Milli-Q ultrapure water (Millipore, Billerica, MA).

The first meconium from healthy term infants was collected from the Kapi'olani Medical Center for Women & Children (Honolulu, HI) and was pooled, lyophilized, and stored at −20°C, following protocols used in the literature (25–27). Before testing, meconium was suspended in the saline buffer and mixed with 5 mg/mL surfactant to yield a final ratio of 1 wt.% and 100 wt.% of the surfactant, respectively.

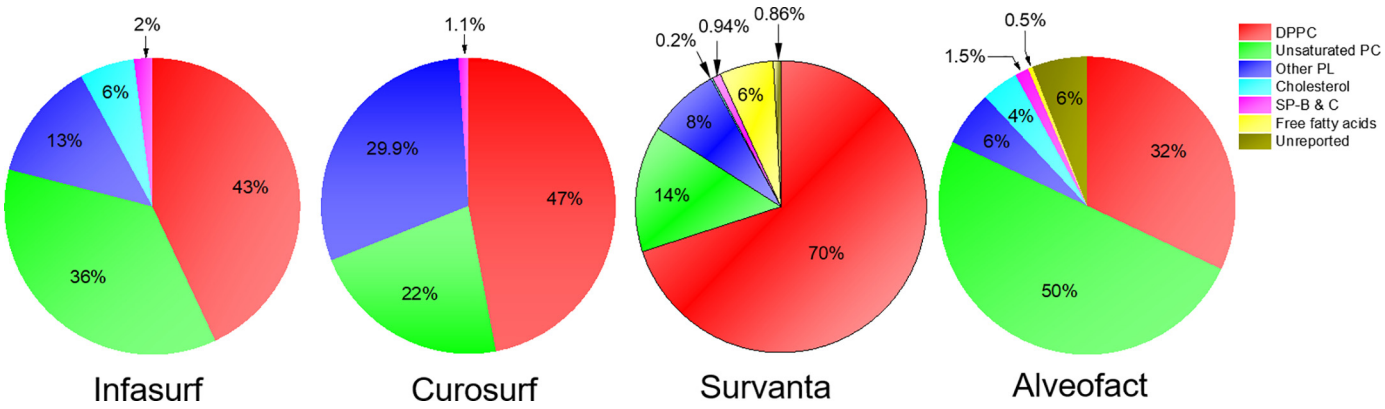


**Figure 1.** Chemical composition of four clinical surfactant preparations: Infasurf, Curosurf, Survanta, and Alveofact. Data represent weight percentage of DPPC, unsaturated PC, phospholipids (PLs) other than PC, neutral lipids (mainly cholesterol), free fatty acids, and combined hydrophobic surfactant proteins SP-B and C (20–24). DPPC, dipalmitoyl phosphatidylcholine; PC, phosphatidylcholine; SP-B and C, surfactant protein B and C.

### Constrained Drop Surfactometry

The CDS is a new generation of droplet-based tensiometry technique developed in our laboratory for biophysical simulations of pulmonary surfactants (15, 16). Detailed schematic description of this device can be found elsewhere (15, 16). In brief, CDS uses the air-water surface of a sessile droplet (~3 mm in diameter, covering an surface area of ~0.14 $cm^2$, and with a volume of around 7 μL) to house the adsorbed surfactant film. The surfactant droplet is securely constrained on a meticulously machined pedestal, featuring knife-sharp edges that prevent film leakage, even at low surface tensions. Periodic compression and expansion of the adsorbed surfactant film at physiologically relevant rates and compression ratios are achieved by controlling liquid flow into and out of the droplet using a motorized syringe. The surface tension and surface area of the adsorbed surfactant film are determined in real-time by analyzing the droplet's shape through closed-loop axisymmetric drop shape analysis (CL-ADSA) (28). Thanks to the miniaturization of the system, CDS enables a high-fidelity simulation of the intra-alveolar environment, maintaining the core body temperature of 37°C and relative humidity close to 100% within an environmental control chamber.

### Subphase Replacement and Langmuir–Blodgett Transfer

To facilitate the direct imaging of the ultrastructure of adsorbed surfactant films, we have developed innovative subphase replacement and in situ LB transfer techniques (19). In brief, the subphase replacement was executed through a coaxial CDS pedestal connected to two motorized syringes. One syringe withdrew the phospholipid-vesicle-containing subphase from the droplet, whereas the other simultaneously injected buffer into the droplet at the same flow rate. The process effectively washed away phospholipid vesicles in the droplet without disturbing the adsorbed surfactant film at the air-water surface. Following the subphase replacement, the LB transfer of the adsorbed surfactant film was conducted by swiftly inserting a freshly peeled mica sheet into the droplet. Subsequently, the mica sheet was gradually lifted across the air-water surface of the droplet at a rate of 1 mm/min.

### Atomic Force Microscopy

The ultrastructure of the adsorbed surfactant films was visualized using an Innova AFM (Bruker, Santa Barbara, CA). Samples were scanned in air using the tapping mode, using a silicon cantilever with a spring constant of 42 N/m and a resonance frequency of 300 kHz. Lateral structures of the surfactant films were analyzed using NanoScope Analysis (v. 1.5).

### Statistics

All results are shown as means ± standard deviation ($n > 3$). Nonparametric Kruskal–Wallis test was used to determine group differences (OriginPro, Northampton, MA). $P < 0.05$ was considered to be statistically significant.

## RESULTS

### Comparison of the Adsorption Rate

Figure 2*A* shows the adsorption isotherms of four clinical surfactants at 1 mg/mL and 37°C. As shown in the *inset* of Fig. 2*A*, all surfactant preparations, except for Survanta, reduce the surface tension of the air-water surface from ~70 mN/m to ~25 mN/m within 10 s, whereas Survanta reduces the surface tension to 41 mN/m after 10 s. The surfactant adsorption becomes substantially slower after the initial 10 s. Within a 5-min period, Infasurf, Curosurf, and Alveofact reach a uniform equilibrium surface tension of 23 mN/m. Survanta only reduces the surface tension to 28 mN/m within the 5-min period. We have extended the observation for Survanta to 10 min, at which point the surface tension is finally reduced to the equilibrium value of ~23 mN/m. During this extended period, the surface area of the surfactant droplet was maintained constant by CL-ADSA to avoid complications introduced by evaporation-induced contraction of the surfactant film (28).

The adsorption kinetics of a surfactant can be qualified by the adsorption time ($\tau_{95}$), i.e., the 95% time required for a surfactant to reduce the surface tension of the air-water surface to its equilibrium value (29). As shown in Fig. 2*B*, $\tau_{95}$ of Infasurf, Curosurf, and Alveofact varies from 4 to 10 s, with Alveofact exhibiting the quickest adsorption. $\tau_{95}$

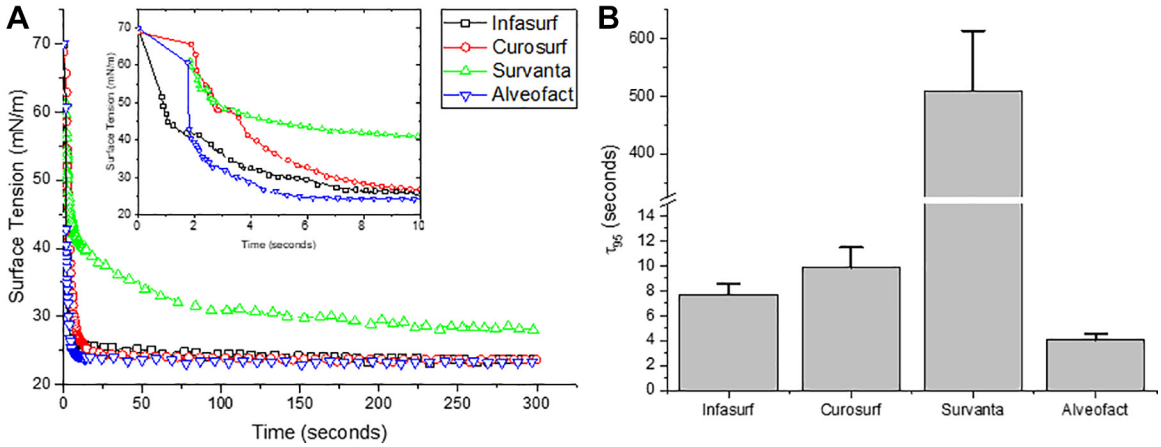


**Figure 2.** Comparative analysis of adsorption rates in four clinical surfactant preparations. *A*: adsorption isotherms of the clinical surfactants at 1 mg/mL and 37°C. The *inset* highlights a rapid reduction in surface tension within the initial 10 s of adsorption. *B*: the time required for 95% adsorption completion ($\tau_{95}$). Significant differences ($P < 0.05$) were observed in comparisons between any two surfactant preparations.

of Survanta is ~510 s, substantially longer than the other clinical surfactants.

### Comparison of the Quasi-Static Surface Activity

Figure 3 depicts the quasi-static surface activity of four clinical surfactants at 37°C. In these biophysical assays, the adsorbed surfactant film underwent quasi-static compression and expansion at a rate of 30 s per cycle, which is 10 times slower than physiologically relevant dynamic cycles. This deliberate slowing of the process in quasi-static assays aims to eliminate kinetic effects associated with dynamic simulations. Throughout the quasi-static cycling, the adsorbed surfactant film at the air-water surface was allowed to relax, efficiently exchanging surface-active materials with those in the subphase, thus entailing the desorption and readsorption of surfactants (30). Compression ratio of the surfactant film ranges from 30% to 50%, ensuring the reach of minimum surface tension ($\gamma_{min}$). The quasi-static surface activity of the surfactant film is directly comparable to the quasi-static surface activity revealed by a Langmuir film balance (30).

Figure 3*A* illustrates the representative quasi-static compression-expansion cycle of four clinical surfactants adsorbed from the surfactant subphase at a phospholipid concentration of 1 mg/mL. The depicted cycle is the fifth cycle following de novo adsorption, with subsequent cycles demonstrating increased reproducibility. At this relatively low concentration, it is evident that both Curosurf and Infasurf can decrease the $\gamma_{min}$ to ~3 mN/m upon quasi-static compression. In contrast, Survanta and Alveofact reach the $\gamma_{min}$ of ~6 and 15 mN/m, respectively (Fig. 3*B*).

The $\gamma_{min}$ alone is not an ideal quantitative criterion for evaluating the biophysical properties of pulmonary surfactant because it is influenced by the compression ratio of the surfactant film. Therefore, we use the average isothermal film compressibility/expandability $\kappa = \frac{1}{A}\left(\frac{\partial A}{\partial \gamma}\right)$ as a metric to compare the biophysical properties of the clinical surfactants. A high-quality surfactant should exhibit low compressibility ($\kappa_{comp}$), meaning it can achieve low surface tensions with only moderate film compression. The expandability ($\kappa_{exp}$) of the surfactant film reflects its stability in overcoming relaxation. An effective surfactant should have an expandability similar to its compressibility, resulting in minimal energy loss per cycle, as indicated by the hysteresis area of the compression-expansion loop. Conversely, a low $\kappa_{exp}$ suggests a rapid increase in surface tension upon film expansion, leading to substantial energy loss per cycle and indicating poor film stability.

The $\kappa_{comp}$ of Infasurf, Curosurf, Survanta, and Alveofact is 2.1, 0.9, 1.9, and 6.4 m/mN, respectively (Fig. 3*C*). Upon quasi-static expansion, the maximum surface tension ($\gamma_{max}$) of these clinical surfactants ranges from 29 (for Alveofact) to 38 mN/m (for Survanta) (Fig. 3*B*). The $\kappa_{exp}$ of Infasurf, Curosurf, Survanta, and Alveofact is 0.6, 0.9, 1.6, and 0.5 m/mN, respectively (Fig. 3*C*). The mismatch between $\kappa_{comp}$ and $\kappa_{exp}$ indicates instability of the surfactant film upon expansion, which leads to energy loss per cycle.

Upon increasing the surfactant concentration to 5 mg/mL, the biophysical properties of Curosurf and Alveofact remain comparable to those at 1 mg/mL. Remarkably, the biophysical properties of Infasurf exhibit significant enhancement, as evidenced by a substantial decrease in $\kappa_{comp}$ and a slight increase in $\kappa_{exp}$ (Fig. 3*F*) compared with the low concentration of 1 mg/mL. The $\kappa_{exp}$ of Survanta, however, decreases to 0.2 m/mN, indicating a less stable film than at 1 mg/mL. This finding is surprising, as an increase in surfactant concentration is typically expected to enhance film stability (31). However, it is worth noting that the high surfactant concentration decreases the $\gamma_{max}$ of Survanta from 38 to 34 mN/m (Fig. 3*E*). Further increasing the surfactant concentration from 5 to 10 mg/mL does not significantly enhance of the biophysical properties of any of these four clinical surfactants (Fig. 3, *G–I*).

### Comparison of the Dynamic Surface Activity

Figure 4 shows the dynamic surface activity of four clinical surfactants at 37°C. In these biophysical assays, the adsorbed surfactant film underwent rapid compression-expansion cycles at a physiologically relevant rate of 3 s per cycle. The compression ratio of the surfactant film spans from 20% to 50%, ensuring the coverage of $\gamma_{min}$ for all clinical surfactants. It is noteworthy, however, that variations in

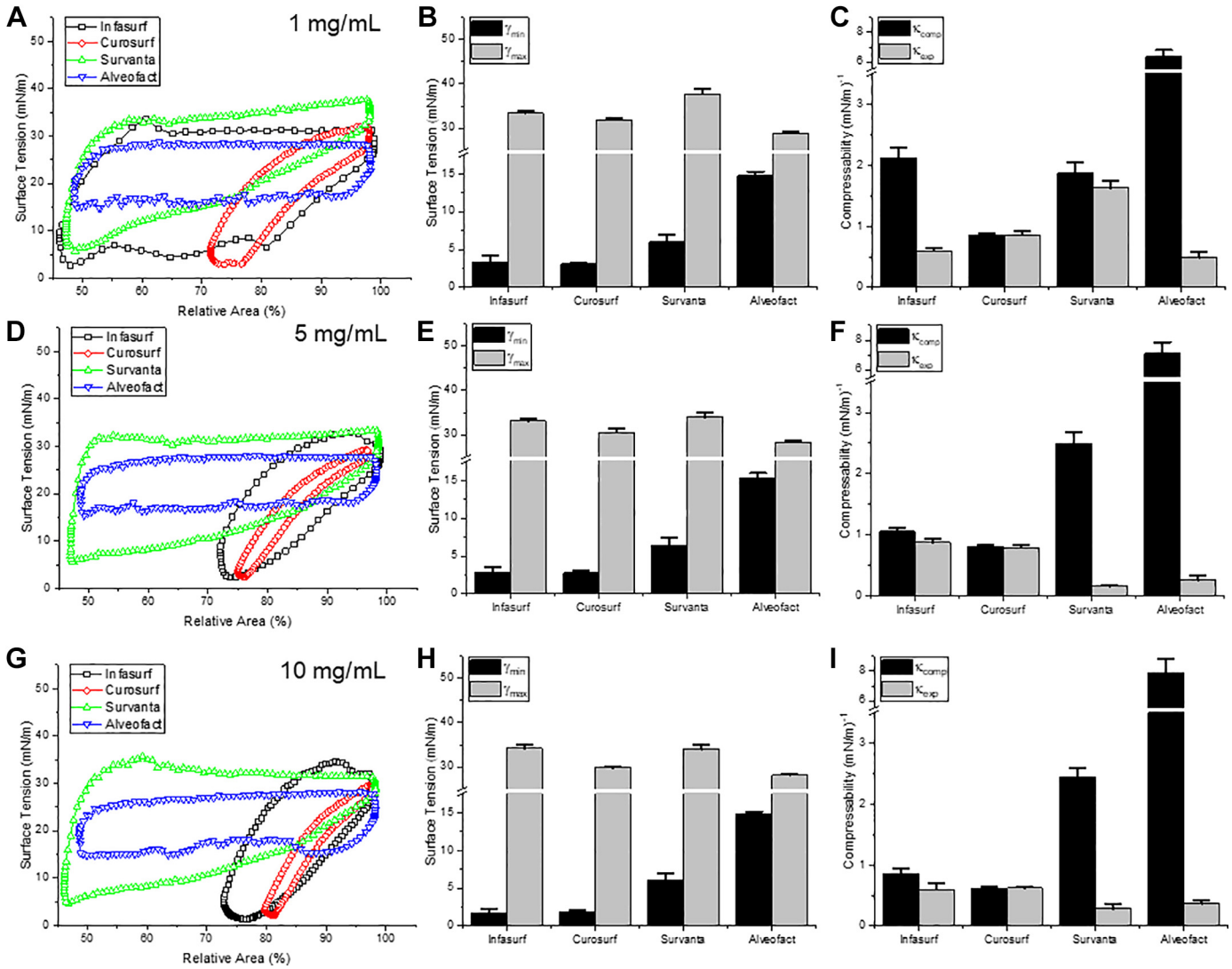


**Figure 3.** Comparative analysis of quasi-static surface activity in four clinical surfactant preparations adsorbed from surfactant concentrations of 1, 5, and 10 mg/mL, respectively, at 37°C. In these biophysical assays, the adsorbed surfactant film underwent quasi-static compression and expansion at a rate of 30 s/cycle. The depicted cycle is the fifth cycle following de novo adsorption, with subsequent cycles demonstrating increased reproducibility. Parameters measured include the minimum ($\gamma_{min}$) and maximum ($\gamma_{max}$) surface tensions, as well as the average film compressibility ($\kappa_{comp}$) and expandability ($\kappa_{exp}$), determined during compression and expansion processes. Significant differences ($P < 0.05$) were observed in comparisons between any two surfactant preparations.

alveolar surface area during normal tidal breathing are likely no more than 20% (32–34). Therefore, the relevance of only the low compression ratio in these biophysical assays lies in their alignment with simulations of normal tidal breathing in humans.

Figure 4*A* shows the representative dynamic compression-expansion cycle of four clinical surfactants adsorbed from a surfactant subphase at a phospholipid concentration of 1 mg/mL. The depicted cycle is the fifth cycle following de novo adsorption, with subsequent cycles demonstrating increased reproducibility. It is evident that Infasurf, Curosurf, Survanta, and Alveofact decrease the $\gamma_{min}$ to 2.3, 2.5, 3.5, and 6.1 mN/m, respectively (Fig. 4*B*). Although all four clinical surfactants reduce the $\gamma_{min}$ to values less than 10 mN/m, only Infasurf and Curosurf achieve these low $\gamma_{min}$ with the physiologically relevant 20% compression ratio, indicated by their low $\kappa_{comp}$, which is less than 0.8 m/mN (Fig. 4*C*). In contrast, Survanta and Alveofact achieve their $\gamma_{min}$ with 30% and 50% compression ratios, respectively. Alveofact exhibits a high $\kappa_{comp}$ of 2.8 m/mN.

Upon expansion of the surfactant films, Infasurf, Curosurf, and Alveofact exhibit similar $\gamma_{max}$ values of 35, 32, and 31 mN/m, respectively (Fig. 4*B*). In contrast, Survanta has the highest $\gamma_{max}$, reaching 46 mN/m, significantly surpassing the $\gamma_{max}$ of 38 mN/m observed for the Survanta film expanded under quasi-static conditions (Fig. 3*B*).

Increasing the surfactant concentration from 1 to 5 and 10 mg/mL progressively enhances the surface activity of Infasurf, Curosurf, and Survanta, but this trend is not observed for Alveofact. At 10 mg/mL, both Infasurf and Curosurf reduce the $\gamma_{min}$ to values less than 3 mN/m with an ~20% compression ratio, whereas Survanta reduces the $\gamma_{min}$ to values less than 5 mN/m with an ~30% compression ratio (Fig. 4, *G–I*). In contrast, the dynamic surface activity of

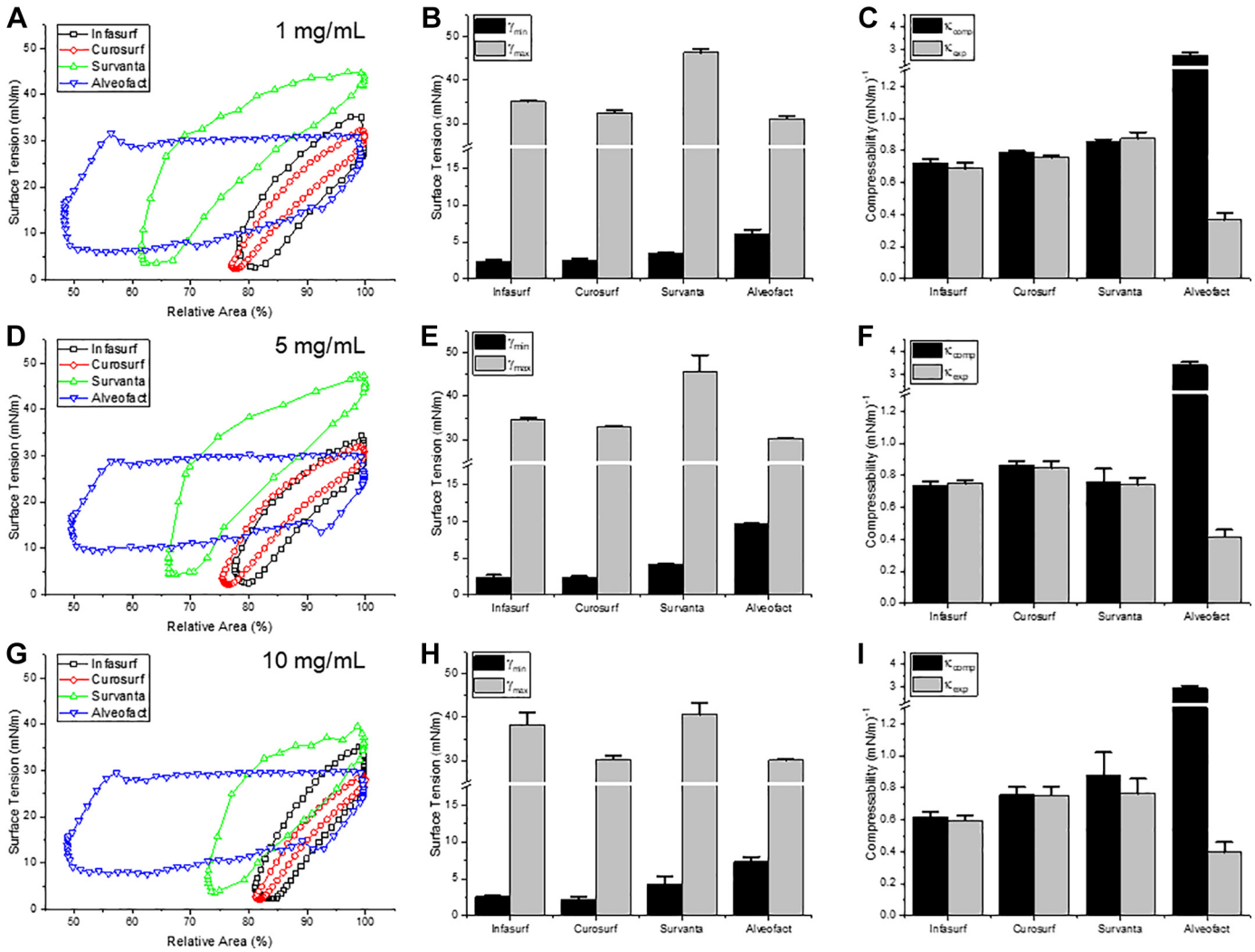


**Figure 4.** Comparative analysis of dynamic surface activity in four clinical surfactant preparations adsorbed from surfactant concentrations of 1, 5, and 10 mg/mL, respectively, at 37°C. In these biophysical assays, the adsorbed surfactant film underwent dynamic compression and expansion at a physiologically relevant rate of 3 s/ cycle. The depicted cycle is the fifth cycle following de novo adsorption, with subsequent cycles demonstrating increased reproducibility. Parameters measured include the minimum ($\gamma_{min}$) and maximum ($\gamma_{max}$) surface tensions, as well as the average film compressibility ($\kappa_{comp}$) and expandability ($\kappa_{exp}$), determined during compression and expansion processes. Significant differences ($P < 0.05$) were observed in comparisons between any two surfactant preparations.

Alveofact remains relatively unchanged compared with lower surfactant concentrations.

### Comparison of the Resistance to Surfactant Inhibition by Meconium

Figure 5 shows the resistance to surfactant inhibition by meconium. Meconium, the first stool of an infant, comprises amniotic fluid, lanugo, cellular debris, and digestive tract byproducts, including the potent digestive surfactants, bile acids, and a significant amount of cholesterol (7, 26). Together with lung inflammation and airway obstruction, surfactant inhibition significantly contributes to the pathophysiology of meconium aspiration syndrome (MAS) (35).

For each clinical surfactant at a concentration of 5 mg/mL, two meconium concentrations (1 and 100 wt% of the surfactant) were investigated. These levels represent the lower and upper bounds of in vitro surfactant inhibition by meconium studied in previous research (25–27). Notably, even 1% meconium induces biophysical inhibition in all four surfactant preparations, as evidenced by elevated $\gamma_{min}$ (Fig. 5*E*) and $\kappa_{comp}$ (Fig. 5*F*). However, distinct differences in surfactant inhibition are observed among these preparations. The introduction of 1% meconium (0.05 mg/mL) raises the $\gamma_{min}$ of Infasurf from 2 to 8 mN/m, Curosurf from 2 to 4 mN/m, Survanta from 4 to 8 mN/m, and Alveofact from 9.5 to 10 mN/m. With 100% meconium (5 mg/mL), $\gamma_{min}$ further increases for Infasurf, Curosurf, Survanta, and Alveofact to 15.5, 7, 14, and 17 mN/m, respectively. Similar trends are observed in $\kappa_{comp}$. These findings suggest that, among the clinical surfactants examined, Curosurf exhibits the highest resistance to biophysical inhibition by meconium.

### Comparison of the Topography and Ultrastructure of Adsorbed Surfactant Films

Figure 6 presents the topography and ultrastructure of surfactant films adsorbed from a subphase concentration of

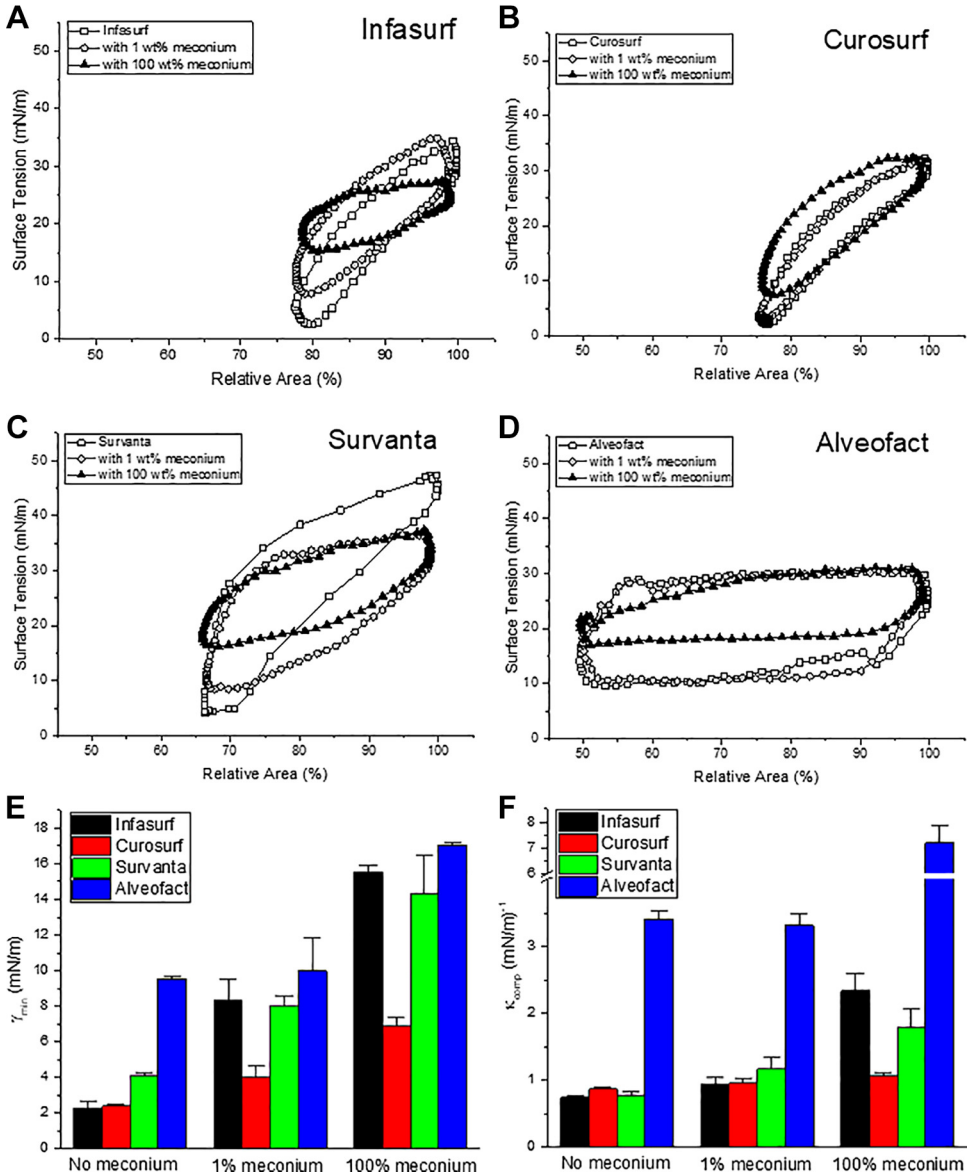


**Figure 5.** Comparative analysis of surfactant resistance to biophysical inhibition by meconium for Infasurf (*A*), Curosurf (*B*), Survanta (*C*), and Alveofact (*D*). Each surfactant, at a concentration of 5 mg/mL, was mixed with 1 and 100 wt% meconium, respectively. The adsorbed surfactant film, with and without the addition of meconium, underwent dynamic compression and expansion at a physiologically relevant rate of 3 s/ cycle at 37°C. The depicted cycle is the fifth cycle following de novo adsorption, with subsequent cycles demonstrating increased reproducibility. *E*: the minimum ($\gamma_{min}$), with (*F*) the average film compressibility ($\kappa_{comp}$). Significant differences ($P < 0.05$) were observed in comparisons between surfactants with and without the addition of meconium.

1 mg/mL and LB transferred at the equilibrium surface tension (23 mN/m) and 37°C. The lateral structure of these clinical surfactant films reveals distinctive topographic features. The adsorbed Infasurf film (Fig. 6*A*) displays uniformly distributed protrusions ranging from 4 to 20 nm in height. With the thickness of a fully hydrated phospholipid bilayer estimated to be around 4 nm (36), these protrusions correspond to 1–5 stacked bilayers, aligning well with our previous observations (16, 19). In contrast to Infasurf, the adsorbed Curosurf film (Fig. 6*B*) exhibits a smaller number of individual larger bilayer protrusions, with isolated high protrusions reaching up to the thickness of three bilayers. The adsorbed Survanta film (Fig. 6*C*) features a network of bilayer protrusions covering the entire film. However, the adsorbed Alveofact film exhibits a topography completely different from the other three clinical surfactants. The adsorbed Alveofact film (Fig. 6*D*) primarily demonstrates a monolayer conformation, with only isolated bilayer protrusions reaching up to 8 nm in height.

## DISCUSSION

### Biophysical Paradox of Pulmonary Surfactant: Soft-Yet-Strong Surfactant Films

A good surfactant preparation should possess at least two fundamental biophysical functions: rapid adsorption/readsorption to the air-water surface, and high metastability upon film compression to very low, near-zero surface tensions (i.e., high surface pressures) (6, 17, 37). These two properties appear contradictory based on classical physicochemical understanding of thin films and monolayers. Fluid unsaturated phospholipids, for instance, adsorb rapidly to the air-water surface, but these films cannot usually sustain the high surface pressures needed for respiration. These phospholipid films tend to collapse whenever compressed beyond the equilibrium spreading pressure of phospholipids (or below the equilibrium surface tension of ~25 mN/m). Conversely, solid disaturated phospholipids, such as DPPC, can sustain surface

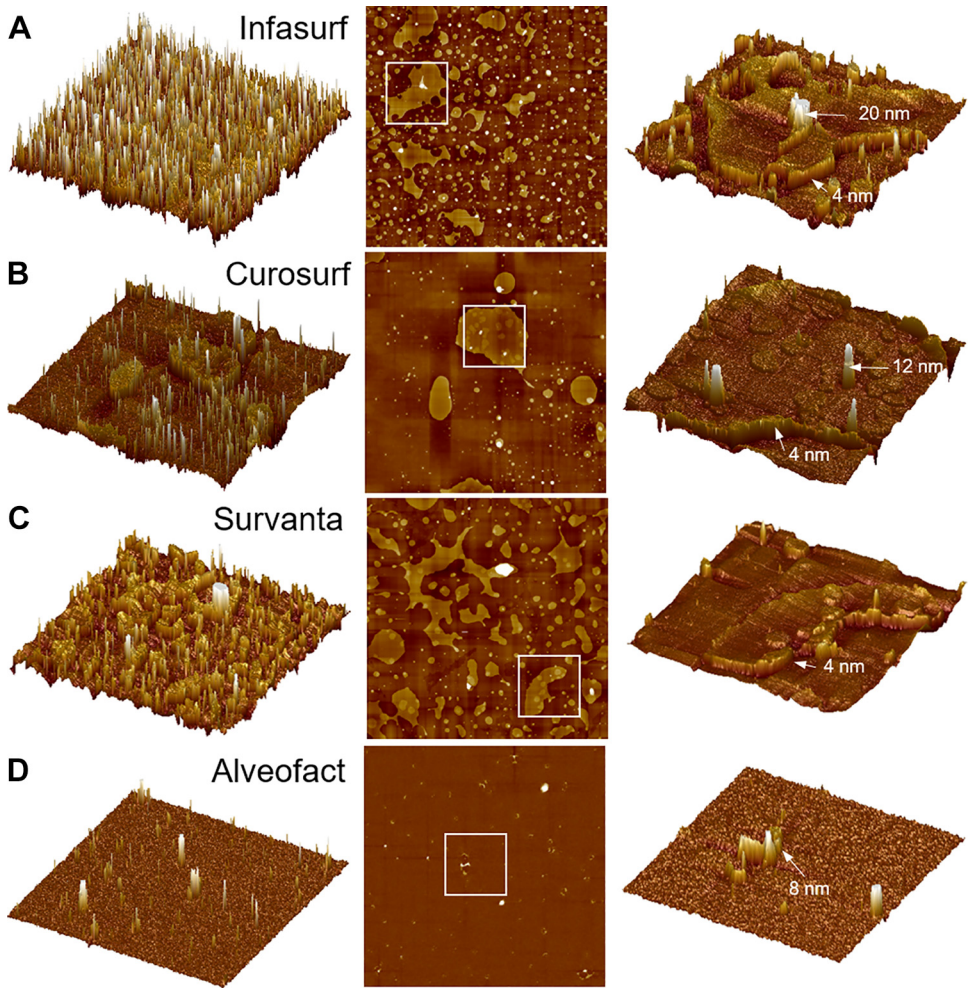


**Figure 6.** *A–D*: comparative analysis of ultrastructure and topography of the adsorbed surfactant films. All surfactant films were adsorbed from a surfactant concentration of 1 mg/mL and Langmuir-Blodgett transferred at the equilibrium surface tension (~23 mN/m) and 37°C. The first and second columns display 3-D rendering and 2-D topography of the adsorption surfactant films, respectively. AFM images cover a 20 × 20 μm scanning area with a *z*-range of 20 nm. The third column highlights the structures within white squares (5 × 5 μm) indicated in the second column. 2-D, two-dimensional; 3-D, three-dimensional; AFM, atomic force microscopy.

pressures significantly higher than equilibrium values without collapsing. However, pure DPPC vesicles adsorb extremely slowly, even at body temperature (38). The mechanism by which pulmonary surfactant resolves this biophysical paradox, forming a soft yet strong film at the alveolar surface to support respiration, remains not fully understood. Available biophysical models for pulmonary surfactants include the classical squeeze-out model, the supercompression model, and the updated adsorption-driven lipid sorting model (17, 37). However, all these models have limitations.

### Composition-Functional Correlations of the Surfactant Films: Effect on Adsorption and Readsorption

By comparing the biophysical properties of four clinical surfactant preparations, we have revealed a surfactant composition-structure-functionality correlation. This correlation could be crucial for understanding the biophysical mechanisms of pulmonary surfactants and for the further development of clinical surfactant preparations.

It was found that the differential adsorption behavior of these clinical surfactants exhibits a clear correlation with their lipid compositions. Illustrated in Fig. 1, DPPC, the disaturated phospholipid, constitutes varying proportions in these clinical surfactants, with Survanta (70%) > Curosurf (47%) > Infasurf (43%) > Alveofact (32%). Being the primary single lipid component in pulmonary surfactant, the adsorption of DPPC in vesicular form is notably sluggish. This fact is underscored by our previous demonstration that the aqueous suspension of DPPC liposomes only reduces surface tension to 40 mN/m after 1 h (38). Similarly, the high fraction of DPPC content is also associated with poor readsorption behavior, especially under highly dynamic compression-expansion cycles. Survanta has the highest $\gamma_{max}$, reaching 46 mN/m, under dynamic conditions (Fig. 4*B*), significantly surpassing the $\gamma_{max}$ of 38 mN/m observed for the Survanta film expanded under quasi-static conditions (Fig. 3*B*). With the supplementation of synthetic DPPC, Survanta demonstrates much higher surface viscosity than other clinical surfactants (21). During rapid expansion, Survanta struggles to replenish the surfactant film, resulting in a surface tension overshoot at the end of expansion and giving rise to a distinctive boomerang-shaped compression-expansion cycle (Fig. 4*A*).

In contrast, the combined portion of unsaturated phosphatidylcholine (PC) and other phospholipid species (most of them are unsaturated) ranks as Alveofact (65%) > Curosurf (52%) > Infasurf (49%) > Survanta (22%). This comparison emphasizes the significance of unsaturated phospholipids, particularly anionic lipids like phosphatidylglycerol (PG) and phosphatidylinositol (PI), in enhancing adsorption kinetics by fluidizing surfactant preparations. Together, PG and PI constitute 10–15 wt% of pulmonary surfactant (39). Literature reports indicate that these anionic lipids play a pivotal role in

regulating the biophysical properties of pulmonary surfactant through interactions with the cationic surfactant proteins, SP-B and SP-C (6, 40, 41).

### Composition-Functional Correlations of the Surfactant Films: Effect on Metastability

Among all studied surfactant preparations, Alveofact is the only clinical surfactant with a DPPC fraction less than 40 wt% (Fig. 1). It is also the only surfactant unable to reduce surface tension below 10 mN/m upon quasi-static compressions (Fig. 3). It should be noted that the quasi-static condition is not physiologically relevant. Under the quasi-static conditions, the surfactant film is compressed and expanded with very low rates, thus eliminating any kinetic effects (30). Under physiologically relevant dynamic conditions, Alveofact can indeed reduce surface tension to below 10 mN/m (Fig. 4).

Hall and coworkers discovered that the metastability of surfactant films is influenced by the rate of compression (42–44). Rapid compression can transform a pulmonary surfactant film, or even a fluid phospholipid film, into a jamming state, mimicking the metastability of disaturated phospholipid films compressed under quasi-static conditions (43). Therefore, surfactant film metastability can be achieved by at least two alternative means: using a surfactant preparation with a significant portion of disaturated phospholipids, mainly DPPC, or compressing the surfactant film at a sufficiently high rate. Our comparative studies indicate that ~40% DPPC may serve as a reasonable lower limit for clinical surfactant preparations to achieve optimal biophysical functionality. Conversely, increasing DPPC content beyond 50%, as seen in Survanta, does not necessarily enhance dynamic surface activity (Fig. 4). Holm et al. (45) demonstrated that further increasing the DPPC content to 60% or 80% in a model system did not improve dynamic surface activity but significantly compromised adsorption. Considering all these factors, our study suggests that a DPPC content of 40%–50% in clinical surfactant preparations may result in the best biophysical properties.

### Structure-Functional Correlations of the Surfactant Films: Monolayer versus Multilayer

In earlier investigations, we compared the lateral structure of clinical surfactant films spread at the air-water surface of a Langmuir film balance (24, 46). These studies revealed that at surface pressures equivalent to the equilibrium surface tension studied here (23 mN/m), the spread films of Infasurf, Curosurf, and Survanta all exhibit a multilayer structure with bilayer protrusions on top of an interfacial monolayer. Similar multilayer structures are observed here for the adsorbed films of these clinical surfactants. A major distinction between these two film formation techniques lies in the fact that the spread film, assisted by a spreading solvent such as chloroform, eliminates the energy barrier for adsorption encountered by the vesicular form of insoluble phospholipids dispersed in the aqueous subphase (38). Therefore, from a technical standpoint, the ultrastructure of the spread film may not entirely reflect the morphology of the in situ pulmonary surfactant film in the lungs. Recent technological advancements in CDS, particularly the subphase replacement technique (19), have facilitated AFM imaging of adsorbed pulmonary surfactant films, offering a more accurate depiction of the surfactant film at the alveolar surface.

Unlike the other clinical surfactants, the adsorbed Alveofact film predominantly exhibits a monolayer conformation. A general consensus is that hydrophobic surfactant proteins, namely SP-B and/or SP-C, are essential for the formation of stable multilayer structures through de novo adsorption (6–8, 17). These hydrophobic proteins, particularly SP-B, play a crucial role in stabilizing a stalk structure that connects the excess phospholipid vesicles with the interfacial monolayer, maintaining a multilayer conformation (47). Consequently, protein denaturation, whether due to exposure to particulate matter (48) or menthol-favored e-cigarette aerosols (49, 50), results in a structural shift of surfactant film from multilayers to monolayers, often associated with a significant inhibition of surfactant's biophysical properties (48–50). Although Survanta contains only one-tenth of SP-B and one-half of SP-C found in natural surfactant, similar to Infasurf and Curosurf, Alveofact contained approximately one-half to one-third of SP-B/C found in natural surfactant (20, 23). Therefore, the unique monolayer conformation and the associated poor surface activity of Alveofact cannot be simply explained by its protein content. In addition, it is noteworthy that among the four clinical surfactants, Alveofact is the only preparation originally formulated in the form of lyophilized dry powder, whereas the other surfactant preparations are dispersed in aqueous suspensions.

### Implications to Surfactant Physiology and Surfactant Therapy

In vitro assays conducted with CDS revealed distinct biophysical properties among four clinical surfactant preparations: Infasurf, Curosurf, Survanta, and Alveofact. At a surfactant concentration of 1 mg/mL, Survanta exhibited a significantly lower adsorption rate compared with the other preparations. Meanwhile, Curosurf demonstrated the superior quasi-static surface activity at the same concentration, as indicated by a significantly lower film compressibility than the other preparations. However, as the surfactant concentration increased to 5 and 10 mg/mL, the differences in quasi-static surface activity between Curosurf and Infasurf diminished. Both Infasurf and Curosurf demonstrated excellent quasi-static surface activity compared with Survanta and Alveofact. Regarding dynamic surface activity, particularly at a physiologically relevant high surfactant concentration of 10 mg/mL, Infasurf, Curosurf, and Survanta all exhibited excellent biophysical properties, characterized by a minimum surface tension of less than 5 mN/m and film compressibility less than 1 m/mN. In contrast, Alveofact displayed the poorest quasi-static and dynamic surface activity among the four clinical surfactants. The adsorbed Alveofact film failed to decrease surface tension below 10 mN/m under quasi-static compressions. Moreover, under the dynamic compression-expansion cycle, although Alveofact could decrease surface tension below 10 mN/m, it requires a 50% film compression, as indicated by notably higher film compressibility compared with the other surfactants. The suboptimal surface activity of Alveofact is found to be correlated with its distinctive monolayer-predominant lateral film structure, whereas other adsorbed surfactant films assume multilayer structures. Regarding resistance to biophysical

inhibition by meconium, it becomes evident that Curosurf outperforms other preparations.

Despite the distinct in vitro biophysical properties of the clinical surfactants studied here, all these animal-derived preparations prove efficacious in treating RDS when administrated in similar doses (51–53). This study specifically focused on animal-derived clinical surfactant preparations authorized for use in the United States and Europe. Among these, Survanta, Infasurf, and Curosurf are approved by the U.S. Food and Drug Administration (FDA) (53), whereas Survanta, Curosurf, and Alveofact are licensed for use in Europe (3). Other animal-derived surfactant preparations, not covered in this study, include bovine lipid extract surfactant (BLES®; BLES Biochemicals, London, ON, Canada) (54), Calsurf (Kelisu; Shuanghe Pharmaceuticals, Beijing, China) (55), Surfacen (Centro Nacional de Sanidad Agropecuaria, Cuba) (56), and goat lung surfactant extract (Cadisurf; Cadila Pharmaceuticals, Ahmedabad, India) (57). In a recent study comparing the clinical and economic efficiency of animal-derived clinical surfactants, including Curosurf, Survanta, Alveofact and BLES, various parameters were analyzed (58). These included the redosing rate, average length of stay, direct medical cost of treatment, medical referral rate, survival at discharge, disability-adjusted life years, and the number of newborns requiring invasive mechanical ventilation. The findings suggested that Alveofact is the least effective surfactant for treating RDS. BLES and Survanta, on the other hand, are the best options for infants with gestation ages above and below 32 wk, respectively (58).

Understanding the differential biophysical behaviors of various clinical surfactants can provide valuable insights into the precision and personalized design of surfactant preparations for the treatment of respiratory diseases beyond RDS. Despite the success of clinical surfactants in treating RDS, their beneficial effects in addressing complications related to surfactant inhibition in neonatal and adult cases, such as MAS (59, 60), acute respiratory distress syndrome (ARDS) (61), and COVID-19 (62, 63), are still under investigation. Moreover, recent studies suggest that clinical surfactants can serve as effective carriers to deliver hydrophobic drugs deep into the lungs (64). For example, clinical surfactants have been explored as a vehicle for delivering corticosteroids to very premature infants with or at a high risk for bronchopulmonary dysplasia (BPD) (65). In vitro biophysical studies indicate that Curosurf, the cholesterol-free preparation, can carry more budesonide than Infasurf, the cholesterol-containing preparation, without significant biophysical inhibition (66, 67).

### Experimental Limitations

It is important to acknowledge the experimental limitations involved in this study, as these limitations may cause deviations between the in vitro biophysical properties and the in vivo clinical performance of the clinical surfactants. First, all four clinical surfactant preparations studied here are recommended to be stored between 2°C and 8°C and are intended for single-time use only. It is well known that storing clinical surfactants at room temperature or higher can cause significant biophysical inhibition (68). In our study, we dispensed the surfactant samples and stored them at their original concentrations at −20°C. Consequently, we did not conduct experiments using surfactant samples from freshly opened, original, nonfrozen vials. Second, the original phospholipid concentrations of Infasurf, Curosurf, Survanta, and Alveofact used in clinical practice are 35, 80, 25, and 45 mg/mL, respectively, which are much higher than the surfactant concentrations (up to 10 mg/mL) studied here. Using CDS, we have studied the biophysical properties of Infasurf at physiologically relevant high surfactant concentrations up to 35 mg/mL (16). It was found that the in vitro dynamic surface activity of Infasurf does not change significantly at phospholipid concentrations beyond 10 mg/mL (16). Third, we did not include a comparative group with unprocessed natural pulmonary surfactants. All animal-derived clinical surfactant preparations differ from natural surfactant in the lack of hydrophilic surfactant proteins (mainly SP-A), significantly reduced levels of hydrophobic proteins (SP-B/C), and variations in certain lipid compositions (e.g., removal of cholesterol from Curosurf and Survanta). It has been found that the quasi-static biophysical properties of bovine natural surfactant at room temperature are indeed superior to those of animal-derived clinical surfactant preparations (24).

In summary, our study involved a thorough investigation into the biophysical properties of four animal-derived clinical surfactant preparations under physiologically relevant conditions, using constrained drop surfactometry. These properties examined included the adsorption rate, quasi-static and dynamic surface activity, resistance to surfactant inhibition by meconium, and the morphology of the adsorbed surfactant films. Through this comparative analysis, we unveiled distinctive in vitro biophysical properties of these clinical surfactants, establishing correlations among their chemical composition, lateral film structure, and biophysical functionality. This understanding of the differential biophysical behaviors of various clinical surfactants provides vital insights for the precision and personalized design of surfactant preparations for the treatment of RDS and beyond. The findings from this study contribute valuable perspectives for the development of more efficacious and fully synthetic surfactant preparations.

## DATA AVAILABILITY

Data will be made available upon reasonable request.

## ACKNOWLEDGMENTS

I thank my former students, Dayne Sasaki and Jinlong Yang, for collecting the experimental data. Special thanks are extended to Dr. Sheree Kuo at the Kapi'olani Medical Center for Women & Children for invaluable assistance in procuring meconium from newborn infants. In addition, I appreciate Dr. Sindhu Row of ONY Biotech for generously providing Infasurf samples, and Dr. Alan Roberts at Cornerstone Therapeutics Inc. for the donation of Curosurf samples.

## GRANTS

This research was supported by the National Science Foundation Grant Nos. CBET-2011317 and CBET-2403397 (to Y.Y.Z.).

## DISCLOSURES

Yi Zuo is an editor of *American Journal of Physiology-Lung Cellular and Molecular Physiology* and was not involved and did not have access to information regarding the peer-review process or final disposition of this article. An alternate editor oversaw the peer-review and decision-making process for this article.

## AUTHOR CONTRIBUTIONS

Y.Y.Z. conceived and designed research; interpreted results of experiments; drafted manuscript; edited and revised manuscript; and approved final version of manuscript.

## REFERENCES


1. **Clements JA**, **Avery ME.** Lung surfactant and neonatal respiratory distress syndrome. *Am J Respir Crit Care Med* 157: S59–S66, 1998. doi:10.1164/ajrccm.157.4.nhlb1-1.
2. **Hallman M**, **Herting E.** Historical perspective on surfactant therapy: transforming hyaline membrane disease to respiratory distress syndrome. *Semin Fetal Neonatal Med* 28: 101493, 2023. doi:10.1016/j.siny.2023.101493.
3. **Sweet DG**, **Carnielli V**, **Greisen G**, **Hallman M**, **Ozek E**, **Te Pas A**, **Plavka R**, **Roehr CC**, **Saugstad OD**, **Simeoni U**, **Speer CP**, **Vento M**, **Visser GHA**, **Halliday HL.** European consensus guidelines on the management of respiratory distress syndrome – 2019 update. *Neonatology* 115: 432–450, 2019. doi:10.1159/000499361.
4. **Ng EH**, **Shah V.** Guidelines for surfactant replacement therapy in neonates. *Paediatr Child Health* 26: 35–49, 2021. doi:10.1093/pch/pxaa116.
5. **Hentschel R**, **Bohlin K**, **van Kaam A**, **Fuchs H**, **Danhaive O.** Surfactant replacement therapy: from biological basis to current clinical practice. *Pediatr Res* 88: 176–183, 2020. doi:10.1038/s41390-020-0750-8.
6. **Pérez-Gil J.** A recipe for a good clinical pulmonary surfactant. *Biomed J* 45: 615–628, 2022. doi:10.1016/j.bj.2022.03.001.
7. **Zuo YY**, **Veldhuizen RA**, **Neumann AW**, **Petersen NO**, **Possmayer F.** Current perspectives in pulmonary surfactant–inhibition, enhancement and evaluation. *Biochim Biophys Acta* 1778: 1947–1977, 2008. doi:10.1016/j.bbamem.2008.03.021.
8. **Rugonyi S**, **Biswas SC**, **Hall SB.** The biophysical function of pulmonary surfactant. *Respir Physiol Neurobiol* 163: 244–255, 2008. doi:10.1016/j.resp.2008.05.018.
9. **Clements J.** Surface tension of lung extracts. *Proc Soc Exp Biol Med* 95: 170–172, 1957. doi:10.3181/00379727-95-23156.
10. **Avery ME**, **Mead J.** Surface properties in relation to atelectasis and hyaline membrane disease. *AMA J Dis Child* 97: 517–523, 1959. doi:10.1001/archpedi.1959.02070010519001.
11. **Clements JA**, **Hustead RF**, **Johnson RP**, **Gribetz I.** Pulmonary surface tension and alveolar stability. *J Appl Physiol* 16: 444–450, 1961. doi:10.1152/jappl.1961.16.3.444.
12. **Schürch S**, **Goerke J**, **Clements JA.** Direct determination of surface tension in the lung. *Proc Natl Acad Sci USA* 73: 4698–4702, 1976. doi:10.1073/pnas.73.12.4698.
13. **Enhorning G.** Pulsating bubble technique for evaluating pulmonary surfactant. *J Appl Physiol Respir Environ Exerc Physiol* 43: 198–203, 1977. doi:10.1152/jappl.1977.43.2.198.
14. **Schürch S**, **Bachofen H**, **Goerke J**, **Possmayer F.** A captive bubble method reproduces the in situ behavior of lung surfactant monolayers. *J Appl Physiol (1985)* 67: 2389–2396, 1989. doi:10.1152/jappl.1989.67.6.2389.
15. **Valle RP**, **Wu T**, **Zuo YY.** Biophysical influence of airborne carbon nanomaterials on natural pulmonary surfactant. *ACS Nano* 9: 5413–5421, 2015. doi:10.1021/acsnano.5b01181.
16. **Xu X**, **Li G**, **Zuo YY.** Constrained drop surfactometry for studying adsorbed pulmonary surfactant at physiologically relevant high concentrations. *Am J Physiol Lung Cell Mol Physiol* 325: L508–L517, 2023. doi:10.1152/ajplung.00101.2023.
17. **Possmayer F**, **Zuo YY**, **Veldhuizen RAW**, **Petersen NO.** Pulmonary surfactant: a mighty thin film. *Chem Rev* 123: 13209–13290, 2023. doi:10.1021/acs.chemrev.3c00146.
18. **Schürch S**, **Bachofen H**, **Possmayer F.** Surface activity in situ, in vivo, and in the captive bubble surfactometer. *Comp Biochem Physiol A Mol Integr Physiol* 129: 195–207, 2001. doi:10.1016/s1095-6433(01)00316-6.
19. **Xu L**, **Yang Y**, **Zuo YY.** Atomic force microscopy imaging of adsorbed pulmonary surfactant films. *Biophys J* 119: 756–766, 2020. doi:10.1016/j.bpj.2020.06.033.
20. **Bernhard W**, **Mottaghian J**, **Gebert A**, **Rau GA**, **von Der HH**, **Poets CF.** Commercial versus native surfactants. Surface activity, molecular components, and the effect of calcium. *Am J Respir Crit Care Med* 162: 1524–1533, 2000. doi:10.1164/ajrccm.162.4.9908104.
21. **Rüdiger M**, **Tölle A**, **Meier W**, **Rustow B.** Naturally derived commercial surfactants differ in composition of surfactant lipids and in surface viscosity. *Am J Physiol Lung Cell Mol Physiol* 288: L379–L383, 2005 [Erratum in *Am J Physiol Lung Cell Mol Physiol* 289: L896, 2005]. doi:10.1152/ajplung.00176.2004.
22. **Blanco O**, **Pérez-Gil J.** Biochemical and pharmacological differences between preparations of exogenous natural surfactant used to treat Respiratory Distress Syndrome: role of the different components in an efficient pulmonary surfactant. *Eur J Pharmacol* 568: 1–15, 2007. doi:10.1016/j.ejphar.2007.04.035.
23. **Notter RH**, **Wang Z**, **Egan EA**, **Holm BA.** Component-specific surface and physiological activity in bovine-derived lung surfactants. *Chem Phys Lipids* 114: 21–34, 2002. doi:10.1016/s0009-3084(01)00197-9.
24. **Zhang H**, **Fan Q**, **Wang YE**, **Neal CR**, **Zuo YY.** Comparative study of clinical pulmonary surfactants using atomic force microscopy. *Biochim Biophys Acta* 1808: 1832–1842, 2011. doi:10.1016/j.bbamem.2011.03.006.
25. **Herting E**, **Rauprich P**, **Stichtenoth G**, **Walter G**, **Johansson J**, **Robertson B.** Resistance of different surfactant preparations to inactivation by meconium. *Pediatr Res* 50: 44–49, 2001. doi:10.1203/00006450-200107000-00010.
26. **Lopez-Rodriguez E**, **Echaide M**, **Cruz A**, **Taeusch HW**, **Perez-Gil J.** Meconium impairs pulmonary surfactant by a combined action of cholesterol and bile acids. *Biophys J* 100: 646–655, 2011. doi:10.1016/j.bpj.2010.12.3715.
27. **Bae CW**, **Takahashi A**, **Chida S**, **Sasaki M.** Morphology and function of pulmonary surfactant inhibited by meconium. *Pediatr Res* 44: 187–191, 1998. doi:10.1203/00006450-199808000-00008.
28. **Yu K**, **Yang J**, **Zuo YY.** Automated droplet manipulation using closed-loop axisymmetric drop shape analysis. *Langmuir* 32: 4820–4826, 2016. doi:10.1021/acs.langmuir.6b01215.
29. **Zuo YY**, **Gitiafroz R**, **Acosta E**, **Policova Z**, **Cox PN**, **Hair ML**, **Neumann AW.** Effect of humidity on the adsorption kinetics of lung surfactant at air-water interfaces. *Langmuir* 21: 10593–10601, 2005. doi:10.1021/la0517078.
30. **Schürch S**, **Green FH**, **Bachofen H.** Formation and structure of surface films: captive bubble surfactometry. *Biochim Biophys Acta* 1408: 180–202, 1998. doi:10.1016/s0925-4439(98)00067-2.
31. **Andreev K**, **Martynowycz MW**, **Kuzmenko I**, **Bu W**, **Hall SB**, **Gidalevitz D.** Structural changes in films of pulmonary surfactant induced by surfactant vesicles. *Langmuir* 36: 13439–13447, 2020. doi:10.1021/acs.langmuir.0c01813.
32. **Bachofen H**, **Schürch S**, **Urbinelli M**, **Weibel ER.** Relations among alveolar surface tension, surface area, volume, and recoil pressure. *J Appl Physiol (1985)* 62: 1878–1887, 1987. doi:10.1152/jappl.1987.62.5.1878.
33. **Bachofen H**, **Schürch S.** Alveolar surface forces and lung architecture. *Comp Biochem Physiol A Mol Integr Physiol* 129: 183–193, 2001. doi:10.1016/s1095-6433(01)00315-4.
34. **Kharge AB**, **Wu Y**, **Perlman CE.** Surface tension in situ in flooded alveolus unaltered by albumin. *J Appl Physiol (1985)* 117: 440–451, 2014. doi:10.1152/japplphysiol.00084.2014.
35. **Osman A**, **Halling C**, **Crume M**, **Al Tabosh H**, **Odackal N**, **Ball MK.** Meconium aspiration syndrome: a comprehensive review. *J Perinatol* 43: 1211–1221, 2023. doi:10.1038/s41372-023-01708-2.
36. **Marsh D.** *CRC Handbook of Lipid Bilayers*. Boca Raton, FL: CRC Press, 1990.
37. **Hall SB**, **Zuo YY.** The biophysical function of pulmonary surfactant. *Biophys J* 123: 1519–1530, 2024. doi:10.1016/j.bpj.2024.04.021.
38. **Bai X**, **Xu L**, **Tang JY**, **Zuo YY**, **Hu G.** Adsorption of phospholipids at the air-water surface. *Biophys J* 117: 1224–1233, 2019. doi:10.1016/j.bpj.2019.08.022.

39. **Markin CJ**, **Hall SB.** The anionic phospholipids of bovine pulmonary surfactant. *Lipids* 56: 49–57, 2021. doi:10.1002/lipd.12273.
40. **Veldhuizen R**, **Nag K**, **Orgeig S**, **Possmayer F.** The role of lipids in pulmonary surfactant. *Biochim Biophys Acta* 1408: 90–108, 1998. doi:10.1016/s0925-4439(98)00061-1.
41. **Ingenito EP**, **Mora R**, **Mark L.** Pivotal role of anionic phospholipids in determining dynamic behavior of lung surfactant. *Am J Respir Crit Care Med* 161: 831–838, 2000. doi:10.1164/ajrccm.161.3.9903048.
42. **Yan W**, **Biswas SC**, **Laderas TG**, **Hall SB.** The melting of pulmonary surfactant monolayers. *J Appl Physiol (1985)* 102: 1739–1745, 2007. doi:10.1152/japplphysiol.00948.2006.
43. **Smith EC**, **Crane JM**, **Laderas TG**, **Hall SB.** Metastability of a supercompressed fluid monolayer. *Biophys J* 85: 3048–3057, 2003 [Erratum in Biophys J 89: 753, 2005]. doi:10.1016/S0006-3495(03)74723-7.
44. **Crane JM**, **Hall SB.** Rapid compression transforms interfacial monolayers of pulmonary surfactant. *Biophys J* 80: 1863–1872, 2001. doi:10.1016/S0006-3495(01)76156-5.
45. **Holm BA**, **Wang Z**, **Egan EA**, **Notter RH.** Content of dipalmitoyl phosphatidylcholine in lung surfactant: ramifications for surface activity. *Pediatr Res* 39: 805–811, 1996. doi:10.1203/00006450-199605000-00010.
46. **Zhang H**, **Wang YE**, **Fan Q**, **Zuo YY.** On the low surface tension of lung surfactant. *Langmuir* 27: 8351–8358, 2011. doi:10.1021/la201482n.
47. **Walters RW**, **Jenq RR**, **Hall SB.** Distinct steps in the adsorption of pulmonary surfactant to an air- liquid interface. *Biophys J* 78: 257–266, 2000. doi:10.1016/S0006-3495(00)76589-1.
48. **Yang Y**, **Xu L**, **Dekkers S**, **Zhang LG**, **Cassee FR**, **Zuo YY.** Aggregation state of metal-based nanomaterials at the pulmonary surfactant film determines biophysical inhibition. *Environ Sci Technol* 52: 8920–8929, 2018. doi:10.1021/acs.est.8b02976.
49. **Goros RA**, **Xu X**, **Li G**, **Zuo YY.** Adverse biophysical impact of e-cigarette flavors on pulmonary surfactant. *Environ Sci Technol* 57: 15882–15891, 2023. doi:10.1021/acs.est.3c05896.
50. **Xu L**, **Yang Y**, **Simien JM**, **Kang C**, **Li G**, **Xu X**, **Haglund E**, **Sun R**, **Zuo YY.** Menthol in electronic cigarettes causes biophysical inhibition of pulmonary surfactant. *Am J Physiol Lung Cell Mol Physiol* 323: L165–L177, 2022. doi:10.1152/ajplung.00015.2022.
51. **Singh N**, **Halliday HL**, **Stevens TP**, **Suresh G**, **Soll R**, **Rojas-Reyes MX.** Comparison of animal-derived surfactants for the prevention and treatment of respiratory distress syndrome in preterm infants. *Cochrane Database Syst Rev* 2015: CD010249, 2015. doi:10.1002/14651858.CD010249.pub2.
52. **Tridente A**, **De Martino L**, **De Luca D.** Porcine vs bovine surfactant therapy for preterm neonates with RDS: systematic review with biological plausibility and pragmatic meta-analysis of respiratory outcomes. *Respir Res* 20: 28, 2019. doi:10.1186/s12931-019-0979-0.
53. **Logan JW**, **Moya FR.** Animal-derived surfactants for the treatment and prevention of neonatal respiratory distress syndrome: summary of clinical trials. *Ther Clin Risk Manag* 5: 251–260, 2009. doi:10.2147/tcrm.s4029.
54. **Yu S**, **Harding PG**, **Smith N**, **Possmayer F.** Bovine pulmonary surfactant: chemical composition and physical properties. *Lipids* 18: 522–529, 1983. doi:10.1007/BF02535391.
55. **Kong X**, **Cui Q**, **Hu Y**, **Huang W**, **Ju R**, **Li W**, **Wang R**, **Xia S**, **Yu J**, **Zhu T**, **Feng Z.** Bovine surfactant replacement therapy in neonates of less than 32 weeks' gestation: a multicenter controlled trial of prophylaxis versus early treatment in China–a pilot study. *Pediatr Neonatol* 57: 19–26, 2016. doi:10.1016/j.pedneo.2015.03.007.
56. **Blanco O**, **Cruz A**, **Ospina OL**, **López-Rodriguez E**, **Vázquez L**, **Pérez-Gil J.** Interfacial behavior and structural properties of a clinical lung surfactant from porcine source. *Biochim Biophys Acta* 1818: 2756–2766, 2012. doi:10.1016/j.bbamem.2012.06.023.
57. **Jain K**, **Nangia S**, **Ballambattu VB**, **Sundaram V**, **Sankar MJ**, **Ramji S et al**. Goat lung surfactant for treatment of respiratory distress syndrome among preterm neonates: a multi-site randomized non-inferiority trial. *J Perinatol* 39: 3–12, 2019. doi:10.1038/s41372-019-0472-0.
58. **Izadi R**, **Shojaei P**, **Haqbin A**, **Habibolahi A**, **Sadeghi-Moghaddam P.** Comparing the clinical and economic efficiency of four natural surfactants in treating infants with respiratory distress syndrome. *PLoS One* 18: e0286997, 2023. doi:10.1371/journal.pone.0286997.
59. **El Shahed AI**, **Dargaville PA**, **Ohlsson A**, **Soll R.** Surfactant for meconium aspiration syndrome in term and late preterm infants. *Cochrane Database Syst Rev* 2014: CD002054, 2014. doi:10.1002/14651858.CD002054.pub3.
60. **Dargaville PA**, **Herting E**, **Soll RF.** Neonatal surfactant therapy beyond respiratory distress syndrome. *Semin Fetal Neonatal Med* 28: 101501, 2023. doi:10.1016/j.siny.2023.101501.
61. **Amigoni A**, **Pettenazzo A**, **Stritoni V**, **Circelli M.** Surfactants in acute respiratory distress syndrome in infants and children: past, present and future. *Clin Drug Investig* 37: 729–736, 2017 [Erratum in Clin Drug Investig 37: 711, 2017]. doi:10.1007/s40261-017-0532-1.
62. **Veldhuizen RAW**, **Zuo YY**, **Petersen NO**, **Lewis JF**, **Possmayer F.** The COVID-19 pandemic: a target for surfactant therapy? *Expert Rev Respir Med* 15: 597–608, 2021. doi:10.1080/17476348.2021.1865809.
63. **Khudadah K**, **Ramadan A**, **Othman A**, **Refaey N**, **Elrosasy A**, **Rezkallah A**, **Heseba T**, **Moawad M**, **Mektebi A**, **Elejla SA**, **Abouzid M**, **Abdelazeem B.** Surfactant replacement therapy as promising treatment for COVID-19: an updated narrative review. *Biosci Rep* 43: BSR20230504, 2023. doi:10.1042/BSR20230504.
64. **Sett A**, **Roehr CC**, **Manley BJ.** Surfactant as a drug carrier. *Semin Fetal Neonatal Med* 28: 101499, 2023. doi:10.1016/j.siny.2023.101499.
65. **Yeh TF**, **Chen CM**, **Wu SY**, **Husan Z**, **Li TC**, **Hsieh WS**, **Tsai CH**, **Lin HC.** Intratracheal administration of budesonide/surfactant to prevent bronchopulmonary dysplasia. *Am J Respir Crit Care Med* 193: 86–95, 2016. doi:10.1164/rccm.201505-0861OC.
66. **Wang YE**, **Zhang H**, **Fan QH**, **Neal CR**, **Zuo YY.** Biophysical interaction between corticosteroids and natural surfactant preparation: implications for pulmonary drug delivery using surfactant as a carrier. *Soft Matter* 8: 504–511, 2012. doi:10.1039/c1sm06444d.
67. **Zhang H**, **Wang YE**, **Neal CR**, **Zuo YY.** Differential effects of cholesterol and budesonide on biophysical properties of clinical surfactant. *Pediatr Res* 71: 316–323, 2012. doi:10.1038/pr.2011.78.
68. **Krill SL**, **Harn J**, **Hahn KR**, **Gupta SL.** Activity loss on room temperature storage of Survanta®, a bovine lung extract based surfactant. *Int J Pharm* 132: 89–94, 1996. doi:10.1016/0378-5173(95)04335-7.